

# ELECTRON-HOLE RECOMBINATION IN IRRADIATED SiO<sub>2</sub> FROM A MICRODOSIMETRY VIEWPOINT

D. B. Brown and C. M. Dozier

*Naval Research Laboratory  
Washington, D. C. 20375*

## ABSTRACT

The fields of radiation chemistry and microdosimetry have produced models for the calculation of the extent of reactions involving radiation-produced ions. This paper presents a model based on ideas developed by Magee and coworkers which are in turn based on the old columnar recombination model of Jaffe. The key contribution of this model is a method for the determination of the spatial distribution of reactants into several differently shaped deposition regions. The implications of this multiple shape recombination (MSR) model for the treatment of electron-hole recombination in MOS oxides will be discussed. In addition, radiation damage in SiO<sub>2</sub> appears to offer a better means for testing such a model than any which has been previously available. That is, the study of electronic devices is benefiting from ideas which originated in the fields of microdosimetry and radiation chemistry, and is in turn providing unique tests of such ideas.

## INTRODUCTION

It has been observed (1,2) that the experimental data for irradiated SiO<sub>2</sub> fits the remarkably simple form

$$N_c^{-1} = A + B \times E^{-1} \quad (1)$$

where  $N_c$  is the number of electron-hole pairs collected,  $A$  and  $B$  are constants, and  $E$  is the field applied across the oxide. That the data should have this form follows directly from a very simple set of assumptions. First, it will be assumed that immediately after the passage of a fast electron there is a cloud of holes and a cloud of electrons which are swept apart in time  $t_r$  by an applied field. Second, it will be assumed that while the electron and hole clouds overlap, electron-hole recombination takes place following bimolecular recombination kinetics, e.g.

$$dR/dt = -\alpha \times R^2, \quad (2)$$

where  $\alpha$  is the recombination coefficient and  $R$  is the hole (and electron) density at time  $t$ . Equation 2 may be solved to obtain

$$1/R_f = 1/R_i + \alpha \times t_r \quad (3)$$

where  $R_i$  is the initial and  $R_f$  is the final hole density. In addition, if it is assumed that

$$t_r = d/(\mu \times E) \quad (4)$$

and that  $N_c$  is proportional to  $R_f$  then the result is essentially the form used by Ausman and McLean (1) where  $d$  is a characteristic length of the reaction volume, and  $\mu$  is the mobility. It will be noted that Eqns. 2-4 contain no terms to account for diffusion of the reactants. This is a reasonable approximation for fields greater than about  $5 \times 10^4$  V/cm (3). The key problem in using Eqns. 3 and 4 is the determination of the size and shape of the reacting volume in order to obtain the characteristic length  $d$ .

Dozier and Brown have presented data on 8080 microprocessors (4) and on MOS capacitors (5) which suggest that the degree of electron-hole recombination in irradiated MOS oxides is dependent on the energy of the irradiating photons. Specifically, they found that <sup>60</sup>Co radiation (about 1 MeV) produced twice the flat band shift per rad as did the radiation from a Cu target x-ray tube (about 10 keV). They felt that the most probable cause for this effect was enhanced electron-hole recombination at the lower energy of the Cu x-ray tube. To restate their hypothesis in terms of Eqns. 3 and 4, they felt that with the Cu tube irradiation,  $R_f/R_i$  was smaller because  $R_i \times d$  was larger.

Mozumder and Magee (6,7) and Magee and Chatterjee (8) have presented calculations (and some data) showing that the relative effectiveness of <sup>60</sup>Co photons and of 1 to 10 keV photons should be significantly different. The work of Magee and coworkers is related to a considerable body of literature in radiation chemistry (9) and radiation dosimetry (10). Their approach has three steps. First, define the stable radiation track types. Second, calculate the fraction of energy which is

deposited into these track entities. Third, treat the recombination kinetics of the various entities assuming bimolecular recombination.

## ENERGY DEPOSITION REGIONS FOR SiO<sub>2</sub>

Mozumder and Magee's definitions of the four track entities will be modified so as to make them appropriate for SiO<sub>2</sub>. For simplicity the colorful names used by Magee and his associates for these four track types will be retained.

1. The "spur": Energetic electrons can undergo energy losses in the 10 to 70 eV range caused by distant encounters resulting in excitons and plasmons. These low-energy loss processes result in average deposition of approximately 40 eV in a roughly spherical region with a radius which Mozumder and Magee estimate to be about 17 Å in H<sub>2</sub>O (7). The work of Ausman and McLean (1) is consistent with a radius of about 60-80 Å in SiO<sub>2</sub>.
2. The "blob": Secondary electrons of approximately 80 to 150 eV can lose energy by ionization leading to tertiary electrons as well as by low energy collective excitations (excitons and plasmons). At such low energies these tertiary electrons will be strongly constrained by Coulomb attraction to the neighborhood of the hole from which they were separated. The cloud of electrons will lose further energy producing spurs. The final result will be a roughly spherical region of overlapping spurs. The radius of this spherical region, the distance beyond which an electron may be taken as free, is such that the energy of the Coulomb attraction is equal to the thermal energy. This radius, the Onsager radius (11), is about 100 Å in SiO<sub>2</sub> at room temperature. The upper limit of 150 eV for the energy of electrons which produce blobs was chosen so that the electron range in SiO<sub>2</sub> (12) is about twice the Onsager radius. Our experience with materials in this atomic number range indicates that few electrons will penetrate farther than about half the electron range (13).
3. The "short track": Secondary electrons of about 150 eV to 5 keV result in short tracks. The path of these electrons is relatively straight (as compared to the electrons forming blobs) because of the relative insignificance of Coulomb attraction by the holes. Energy loss in short tracks is handled in three parts. The portion of the energy lost to low energy collective interactions (about 1/2 the energy) results in a roughly cylindrical column of overlapping spurs. In this simple picture the radius of the cylindrical column is about equal to the radius of its constituent spurs. The portion of the energy lost to high energy knock-on collisions is treated as independent short tracks. The end of a short track, where the electron energy drops below 150 eV, is treated as a blob.
4. The "branch track": Secondary electrons with greater than about 5 keV result in branch tracks. These are similar to short tracks, but with the important difference that the spurs caused by low energy collective excitations are not overlapping. The lower limit of 5 keV was chosen to make the mean distance between spurs a few times the initial size of the spurs. The end of the branch track, where the electron energy drops below 5 keV, is treated as a short track.

## ENERGY DEPOSITION IN SiO<sub>2</sub>

The recombination kinetics will be different in isolated spurs, blobs, and the columnar region of short tracks because of the difference in the amount of spur overlap and the different shape of the recombining volumes. Thus the next step is to show that the initial electrons from <sup>60</sup>Co (order of 500 keV) and the initial electrons produced by Cu tube

x-rays (order of 7 keV) lead to differing fractions of energy deposited in isolated spurs, blobs, and the columnar region of short tracks. Calculations supporting such a conclusion have previously been done for irradiation of water, notably by Mozumder and Magee (6) and by Hamm et al. (14).

A summary of such a calculation for SiO<sub>2</sub> will be given based on a simple algorithm of Mozumder and Magee (6). This algorithm has two parts. For a given electron energy, first calculate the fraction of energy going to high energy knock-on processes (energy losses of greater than 100 eV.) Mozumder and Magee give a formula for this fraction (6). It is about 50% at low energies and drops only slightly to 34% at 10 MeV. Secondly, for knock-on collisions, assume as an approximation the Ruth-erford cross section,

$$w(E_2) = E_2^{-1} \quad (5)$$

where  $w(E_2)$  is the fraction of energy lost per unit energy interval to produce secondary electrons of energy  $E_2$ . From this it follows that equal energy is lost per equal logarithmic energy interval. Such a rule can be applied systematically to obtain the energy deposited as isolated spurs, blobs and the columnar region of short tracks. Figure 1 presents the results of such a calculation. Note that for initial electron energies of above 15 keV the energy is predominantly deposited in isolated spurs. Similarly, the 1-10 keV region is dominated by deposition in the columnar region of short tracks, and below 400 eV deposition is predominantly in blobs.

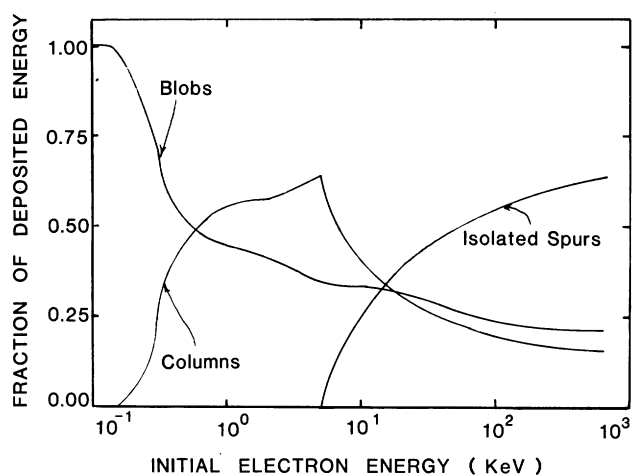


Fig. 1 — The fraction of energy which is deposited as isolated spurs, columns, and blobs.

### RECOMBINATION IN SiO<sub>2</sub>

Finally, the above calculations for SiO<sub>2</sub> will be used to estimate the degree of electron-hole recombination as a function of the incident energy of the irradiating photons. Recombination will be handled using the simple model implied by Eqns. 3 and 4. This is equivalent to the high field limit of the Jaffe model (15), as used by Ausman and McLean (1), with two modifications. First, spherical (spurs and blobs) and columnar energy deposition regions will be treated; the Jaffe model uses only columnar regions. Second, a constant initial hole density within our energy deposition regions will be assumed; the Jaffe model uses a Gaussian distribution of ionic densities. Mozumder and Magee (7) state that the sharp boundary and Gaussian approximations lead to the same result if the parameters are appropriately chosen.

The calculations have been performed using a mobility of 20 cm<sup>2</sup>/(V·sec) from Hughes (16), a recombination coefficient of  $1 \times 10^{-5}$  cm<sup>3</sup>/sec from Hughes (17), and an effective energy to produce an electron-hole pair of 16 eV from Ausman and McLean (1). For recombination within blobs the blob radius,  $r_{\text{blob}}$  was taken to be 100 Å, the Onsager radius for SiO<sub>2</sub>. The characteristic length  $d$  to be inserted in Eqn. 4 was specified by

$$d_{\text{blob}} = ((4/3)\pi)^{1/3} r_{\text{blob}} \quad (6)$$

For recombination within columns a column radius of 100 Å was used. This value was obtained by a fit to experimental data in the 1-10 keV

region. This fit will be shown in Fig. 3 below. Also, the characteristic length was given by

$$d_{\text{column}} = (\pi/2)(\pi)^{1/2} r_{\text{column}} \quad (7)$$

The initial factor of  $\pi/2$  in Eqn. 7 is to allow for the fact that the field may take all angles with respect to the cylinder axis with equal probability. Column lengths were obtained using the electron ranges in SiO<sub>2</sub> of Tung et al. (12). For recombination within spurs a spur radius of 100 Å was used, that is, the spur radius was set equal to the cylinder radius. Also, the characteristic length was given by

$$d_{\text{spur}} = ((4/3)\pi)^{1/3} r_{\text{spur}} \quad (8)$$

Finally, the average energy deposited within a spur was assumed to be 30 eV. This value was obtained by a fit to experimental data in the 15 keV to 500 keV region. This fit will be shown in Fig. 3 below.

Figure 2 shows calculated values of the fraction of electron-hole pairs escaping recombination for fields between  $10^5$  and  $3 \times 10^6$  V/cm and for initial electron energies of 2, 7 and 500 keV. Figure 3 shows similar calculations for a field of  $3 \times 10^5$  V/cm and for initial electron energies of 100 eV to 500 keV. The solid squares in Fig. 3 represent the experimental data of Dozier and Brown (5,18). These experimental results were taken using photon irradiation with photon energies between 70 eV (synchrotron radiation) and 1.25 MeV (<sup>60</sup>Co). The intermediate values were taken using radiation which was predominantly the K shell characteristic lines of Al, Cu, and Mo. In each case these experimental data have been plotted at an energy which approximately represents the energy of the initial electrons generated by photon interaction with the SiO<sub>2</sub>.

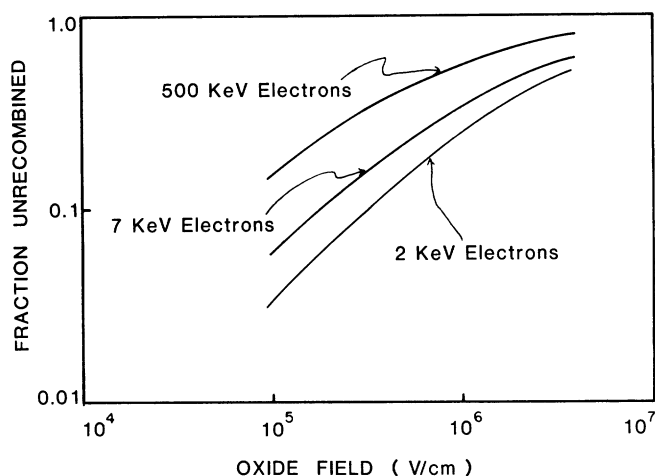


Fig. 2 — The fraction of electron-hole pairs escaping recombination as a function of field in the oxide.

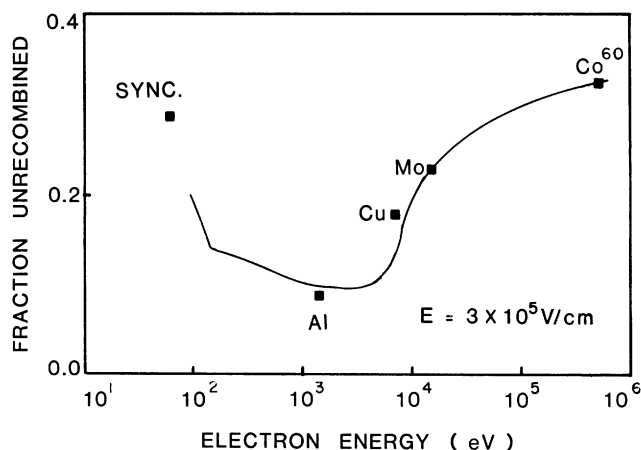


Fig. 3 — The fraction of electron-hole pairs escaping recombination versus initial electron energy. The squares show the experimental data of Dozier and Brown (18).

## DISCUSSION

It is clear from the comparison between calculation and experiment given in Fig. 3 that a multiple shape recombination (MSR) model of the form introduced in this paper can be made to fit experimental data for recombination in SiO<sub>2</sub> using reasonable values for the necessary physical parameters.

Ausman and McLean have fit a purely columnar recombination model to the experimental data of Curtis et al. (19). They obtained a fit to that data (using electron energies in the 1-10 keV range) with  $b = 65.6 \text{ \AA}$  or  $b = 81.3 \text{ \AA}$  (depending on the data). A comparison of Eqns. 3, 4, and 7 with Eqn. 4 of reference 1 gives

$$r_{\text{column}} = 2^{3/2}b. \quad (9)$$

Thus, in the terminology of the present paper, Ausman and McLean find column radii of 185 Å and 230 Å. This is substantially larger than the 100 Å found using the MSR model. The reason for this fact is that in the 1-10 keV range the MSR model predicts that about 40% of the energy is deposited in blobs, and that these blobs have a lower recombination rate than that which is found in columns. For example, for 5 keV electrons and a field of  $3 \times 10^5$  the fraction of electron-hole pairs escaping recombination is calculated to be 7.6% for columns and 15.2% for blobs. If the MSR model had been restricted to energy deposition only in columns a larger column radius would have been required in order to fit experimental data.

In addition, Oldham and McGarrity (20) have fit a columnar recombination model to recombination data for ionization by  $\alpha$  particle and proton irradiation. They find  $b = 40 \text{ \AA}$  for  $\alpha$  particles and  $b = 30 \text{ \AA}$  for protons. In the terminology of the present paper these correspond to column radii of 85-113 Å. From this it may be inferred that the column radius (and thus the spur radius) is nearly the same for ionizing tracks due to electrons,  $\alpha$  particles, and protons.

The average energy deposited within one spur which was found to match experimental results (in Fig. 3) was about 30 eV. This may be compared with the plasmon energy in SiO<sub>2</sub> of 22.4 eV (1). It may also be compared with the data for the energy loss function  $\text{Im}(-1/\epsilon)$  given in Fig. 2 of the paper of Ashley and Anderson (21). It appears very much as if spur is to be associated with one (or perhaps two) plasmons. However, it is perhaps preliminary to make such an association.

The MSR model for recombination in SiO<sub>2</sub> appears to be qualitatively correct, but is sufficiently phenomenological to encourage some doubt about its quantitative predictions. It is hoped in the near future to obtain experimental results in the 100 eV to 1 keV range. If such results should fall in line with the predictions of Fig. 3 it would give additional assurance of the fundamental correctness of the model.

## REFERENCES

1. G. A. Ausman Jr. and F. B. McLean, *App. Phys. Lett.* **26**, 173 (1975).
2. C. M. Dozier, unpublished work.
3. The reasoning leading to this conclusion can be found in M. Schott, *Mol. Cryst. Liq. Cryst.* **10**, 399 (1970).
4. C. M. Dozier, D. B. Brown and J. W. Sandelin, *IEEE Trans. Nuc. Sci.*, NS-27, 1299 (1980).
5. C. M. Dozier and D. B. Brown, *IEEE Trans. Nuc. Sci.*, NS-27, 1694 (1980).
6. A. Mozumder and J. L. Magee, *Rad. Res.* **28**, 203 (1966).
7. A. Mozumder and J. L. Magee, *Rad. Res.* **28**, 215 (1966).
8. J. L. Magee and A. Chatterjee, *J. Phys. Chem.* **82**, 2219 (1978).
9. A. Hummel in *Advances in Radiation Chemistry*, Vol. 4, M. Burton, and J. L. Magee, Eds. (Wiley-Interscience, New York, 1974) p. 2 ff.
10. J. W. Boag in *Radiation Dosimetry*, Vol. II, F. H. Attix and W. C. Roesch, Eds. (Academic Press, New York, 1966) pp. 11-36.
11. L. Onsager, *Phys. Rev.* **54**, 554 (1938).
12. C. J. Tung, J. C. Ashley, V. E. Anderson, and R. H. Ritchie, *RADC Tech. Rept. No. RADC-TR-125*, April 1976.
13. See for example D. B. Brown, D. B. Wittry, and D. F. Kyser, *J. Appl. Phys.* **40**, 1628 (1969).
14. R. N. Hamm, H. A. Wright, J. E. Turner, and R. H. Ritchie, in *Sixth Symposium on Microdosimetry, Brussels, Belgium, May 22-26, 1978*, J. Booz and H. G. Ebert, Eds. (Harwood Academic Publishers) p. 179.
15. G. Jaffe, *Ann. Phys. (Leipz.)* **42**, 303 (1913); also, the Jaffe model is reviewed in references 9 and 10.
16. R. C. Hughes, *Phys. Rev. Lett.* **30**, 1333 (1973).
17. R. C. Hughes, *Solid State Electronics* **21**, 251 (1978).
18. C. M. Dozier and D. B. Brown, this issue.
19. O. L. Curtis Jr., J. R. Srouf, and K. Y. Chiu, *J. Appl. Phys.* **45**, 4506 (1974).
20. T. R. Oldham and J. M. McGarrity, this issue.
21. J. C. Ashley and V. E. Anderson, this issue.